THE JOURNAL OF BIOLOGICAL CHEMISTRY VOL. 285, NO. 21, pp. 16206–16217, May 21, 2010
Printed in the U.S.A.

Embryonic Expression of Cyclooxygenase-2 Causes Malformations in Axial Skeleton*[S]

Received for publication, October 23, 2009, and in revised form, March 10, 2010 Published, JBC Papers in Press, March 17, 2010, DOI 10.1074/jbc.M109.078576

Minsub Shim[‡], Julie Foley[§], Colleen Anna[‡], Yuji Mishina[¶], and Thomas Eling[‡1]

From the [‡]Laboratory of Molecular Carcinogenesis and [§]Cellular and Molecular Pathology Branch, NIEHS, National Institutes of Health, Research Triangle Park, North Carolina 27709 and the [¶]Department of Biologic and Materials Science, School of Dentistry, University of Michigan, Ann Arbor, Michigan 48109-1078

Cyclooxygenases (COXs) have important functions in various physiological and pathological processes. COX-2 expression is highly induced by a variety of stimuli and is observed during certain periods of embryonic development. In this report, the direct effect of COX-2 expression on embryonic development is examined in a novel COX-2 transgenic mouse model that ubiquitously expresses human COX-2 from the early stages of embryonic development. COX-2 transgenic fetuses exhibit severe skeletal malformations and die shortly after birth. Skeletal malformations are localized along the entire vertebral column and rib cage and are linked to defective formation of cartilage anlagen. The cartilage anlagen of axial skeleton fail to properly develop in transgenic embryos because of impaired precartilaginous sclerotomal condensation, which results from the reduction of cell number in the sclerotome. Despite the ubiquitous expression of COX-2, the number of apoptotic cells is highly increased in the sclerotome of transgenic embryos but not in other tissues, suggesting that it is a tissue-specific response. Therefore, the loss of sclerotomal cells due to an increased apoptosis is probably responsible for axial skeletal malformations in transgenic fetuses. In addition, the sclerotomal accumulation of p53 protein is observed in transgenic embryos, suggesting that COX-2 may induce apoptosis via the up-regulation of p53. Our results demonstrate that the aberrant COX-2 signaling during embryonic development is teratogenic and suggest a possible association of COX-2 with fetal malformations of unknown etiology.

Cyclooxygenase (COX)[2] is a rate-limiting enzyme in the arachidonic acid cascade and catalyzes the conversion of arachidonic acid to prostaglandin H_2, which is then converted to various prostaglandins by cell-specific prostaglandin synthases. There are two isoforms of cyclooxygenase. COX-1 (cyclooxygenase-1) is constitutively expressed in many tissues and is thought to play roles in tissue homeostasis. COX-2 (cyclooxygenase-2) has a low level of basal expression in most tissues and cell types. However, its expression is highly inducible by many stimuli, such as cytokines, growth factors, and xenobiotics. Normally, COX-2 expression returns to basal levels after the termination of the stimulus. However, its expression remains high with a persistent stimulus, such as an exposure to xenobiotics or chronic inflammation. Indeed, an increased level of COX-2 is frequently observed in various diseases or pathological conditions, and several COX-2 transgenic mouse models have elucidated the role of COX-2 and its downstream signaling pathways.

Despite the well known functions of COX-2, its role during embryonic development has not been studied in detail. COX-2 expression is observed in rat fetal organs, including skin, heart, cartilage, and kidney, during gestation days 15–20 (1). COX-2 knock-out mice exhibit developmental defects, such as patent ductus arteriosus (2), indicating that the regulation of COX-2 expression is important in embryonic heart development. In addition, several animal studies have suggested a possible role for COX-2 in teratogen-induced embryonic malformation. COX-2 may be associated with the teratogenic effect of benzo(a)pyrene (3), and the teratogenic effect of alcohol is antagonized by the administration of COX inhibitors (4, 5). Furthermore, COX-2 expression is induced during infection and inflammation, which may be associated with unfavorable fetal outcomes. However, the direct effects of COX-2 expression on embryonic malformation have never been determined.

Therefore, we hypothesized that COX-2 expression in critical periods may interfere with embryonic development. A COX-2 transgenic mouse model developed using a Cre-*lox*P system allowed us to investigate the direct effects of aberrant COX-2 expression during embryonic development. In this report, we show that transgenic expression of COX-2 interferes with normal embryonic development, resulting in a severely malformed axial skeleton.

EXPERIMENTAL PROCEDURES

Generation of COX-2 Transgenic Mice—The transgenic basic cassette, pCAG-CAT-HES-poly(A), was a gift from Dr. Junichi Miyazaki (Osaka University Medical School, Japan). Human *COX-2* cDNA was inserted into HindIII and EcoRV sites of pCAG-CAT-HES-poly(A). The transgenic vector was digested with SalI and PstI to remove the vector region. The insert fragment was recovered from the gel and diluted to 2 μg/ml concentration in 1 mM Tris/HCl (pH 8.0) and 0.1 mM EDTA. The

* This work was supported, in whole or in part, by the National Institutes of Health, NIEHS, Intramural Research Program.

[S] The on-line version of this article (available at http://www.jbc.org) contains supplemental Figs. 1–4.

[1] To whom correspondence should be addressed: Laboratory of Molecular Carcinogenesis, NIEHS, National Institutes of Health, 111 TW Alexander Dr., Research Triangle Park, NC 27709. Tel.: 919-541-3911; Fax: 919-541-0146; E-mail: eling@niehs.nih.gov.

[2] The abbreviations used are: COX, cyclooxygenase; CAG, cytomegalovirus early enhancer/chicken β-actin; CAT, chloramphenicol acetyltransferase; TUNEL, terminal dUTP nick end labeling; CT, computed tomography; E*n*, embryonic day *n*.

DNA fragment was introduced into pronuclei of 0.5-day mouse embryos (B6D2F1, Taconic) by glass capillaries. Injected embryos were cultured in KSOM (Sigma) for 1 day, and embryos that reached the two-cell stage were transferred into oviducts of pseudopregnant females (Swiss, Taconic). The offspring were initially screened by PCR for the choramphenicol acetyltransferase (CAT) gene from tail tissue (CAT2 primer, 5′-CAGTCAGTTGCTCAATGTACC-3′; CAT3 primer, 5′-ACTGGTGAAACTCACCCA-3′). For production of the *CAT*^{fl}*COX2* mice, five lines were initially established, and two of them, lines 12 and 17, showing high CAT activity in liver, were chosen for further analysis. A *Mox2-Cre* female (or *CAT*^{fl}*COX2* female) mouse was housed overnight with a *CAT*^{fl}*COX2* male (or *Mox2-Cre* male) mouse. The presence of a vaginal plug the next morning was designated as gestational day 0, and females with a vaginal plug were weighed. At the time of collection, females were weighed again, and pregnancy was confirmed by weight gain. All mouse experiments were performed in accordance with NIEHS/National Institutes of Health guidelines covering the humane care and use of animals in research.

Genotyping—Genomic DNA was isolated from embryonic yolk sacs (E9.5–E13.5) and from tails (E18.5) using a DNeasy kit (Qiagen). Isolated genomic DNA was amplified using ExTaq DNA polymerase (Takara) with a primer set designed to detect the presence of a recombined human *COX-2* allele (forward primer, 5′-GTGCTGGTTATTGTGCTGTCTC-3′; reverse primer, 5′-TCTCCATAGAATCCTGTCCGGGTA-3′), and PCR products were run on 1.2% agarose gel. The recombined human *COX-2* allele was identified as a ~300-bp PCR product, whereas the non-recombined human *COX-2* allele was identified as a ~1.8-kb fragment. For the presence of the *Cre* gene, genomic DNA was amplified by PCR using a primer set for *Cre* (forward primer, 5′-ACCTGAAGATGTTCGCGATTATCT-3′; reverse primer, 5′-ACCGTCAGTACGTGAGATATCTT-3′).

Immunohistochemistry—E9.5–E13.5 embryos were isolated and fixed in 4% paraformaldehyde in phosphate-buffered saline overnight at 4 °C and stored in 70% ethanol at 4 °C until use. E18.5 fetuses were fixed in 10% neutral buffered formalin and stored in 70% ethanol. Fixed embryos were embedded in paraffin block, and paraffin sections were deparaffinized and hydrated. Antigen retrieval was performed by immersing sections in 10 mM sodium citrate (pH 6.0) at 95 °C for 30 min. Sections were incubated with primary antibody (human COX-2 (1:500), Cayman; *Col2a1* (1:100), LabVision; phosphohistone H3 (Ser^{10}) (1:1000), Millipore; cleaved caspase-3 (1:250), Cell Signaling; p53 (1:1000), Novocastra) at 4 °C overnight. Washed sections were incubated in ImmPress reagent (Vector Laboratories) for 30 min and visualized with diaminobenzidine.

Whole Mount in Situ Hybridization and Whole Mount TUNEL Staining—E9.5 or E10.5 embryos were isolated from pregnant female mice by cesarean section, and the yolk sac from each embryo was taken for genotyping. Isolated embryos were fixed in 4% paraformaldehyde in phosphate-buffered saline overnight at 4 °C. Fixed embryos were dehydrated with PBT (phosphate-buffered saline and 0.1% Tween 20) and graded methanol and then stored in methanol at −20 °C until use. Probes for hybridization were amplified by PCR from cDNA generated from E10.5 mouse embryo RNA using the following primers (*Uncx4.1*, 5′-CTCGGTGCCCTTCTCCATCGA-3′ and 5′-GAGCGATCTCCTCTGGGTCCA-3′; *Myogenin*, 5′-GAGAAGCGCAGGCTCAAGAAAGTGA-3′ and 5′-GGCTGTTTTCTGGACATCAGGACA-3′; *Pax1* (paired box 1), 5′-CACGTCAGTATCCCGCGTTCAT and 5′-TCCGTGTAAGCTACCGAGTGCA-3′; *Sox9* (SRY-box9), 5′-GGTGAAGAACGGACAAGCGGA-3′ and 5′-GCTGCTTCGACATCCACACGT-3′). The amplified PCR product was ligated into pSPT18 (Roche Applied Science) and verified by sequencing. Digoxigenin-labeled antisense RNA probes were generated using a digoxigenin labeling kit (Roche Applied Science) according to the manufacturer's protocol. For whole mount TUNEL staining, rehydrated embryos were treated with 10 μg/ml proteinase K in PBT for 10 min at 37 °C and incubated in reaction mixture (1× TdT buffer (Roche Applied Science), 0.5 μM digoxigenin-dUTP, 40 μM dTTP, 12.5 units/ml TdT) for 2 h at 37 °C. After overnight incubation in anti-digoxigenin-alkaline peroxidase-conjugated antibody (Roche Applied Science) at 4 °C, TUNEL-positive cells were visualized in nitro blue tetrazolium/5-bromo-4-chloro-3-indolyl phosphate solution (Roche Applied Science).

Western Blot Analysis—Tissues from E18.5 fetuses were lysed in radioimmune precipitation buffer, and protein concentration was measured using a BCA protein assay kit (Pierce). Equal amounts of protein were heated at 65 °C in LDS sample buffer (Invitrogen) with sample reducing agent (Invitrogen) for 10 min and then separated by SDS-PAGE. The separated proteins were transferred to an Immobilon-P membrane (Millipore). Following incubation in blocking buffer (TBS with 5% nonfat dry milk and 0.1% Tween 20) for 1 h at room temperature, the membranes were probed overnight at 4 °C. The membranes were washed and then probed with a horseradish peroxidase-linked secondary antibody (Amersham Biosciences) for 1 h at room temperature. Detection was made with an enhanced chemiluminescence reagent (Amersham Biosciences), followed by exposure of membrane to film.

Skeletal Preparation—At E18.5, a pregnant female mouse was sacrificed by CO_2 asphyxiation followed by cervical dislocation. Fetuses were isolated by cesarean section and euthanized by hypothermia. Fetuses were scalded in hot tap water for 25 s, and epidermis was removed using a cotton tip applicator. Internal organs, muscle, eyes, and fat were removed, and embryos were fixed in 95% ethanol for 5 days at −20 °C. Embryos were stained with Alcian blue staining solution (0.15% Alcian blue 8GX (Sigma), 20% glacial acetic acid in 95% ethanol) overnight at 37 °C. Stained fetuses were washed with 95% ethanol for 1 h and incubated in Alizarin red staining solution (0.0025% Alizarin red (Sigma) in 1% KOH) for 6 h at room temperature. Stained fetuses were cleared in 1% KOH and graded glycerol and then stored in glycerol.

For Alcian blue cartilage staining, E13.5 embryos were isolated and fixed in Bouin's solution (Poly Scientific) for 2 h and rinsed with 70% ethanol plus 0.1% NH_4OH. Embryos were stained in Alcian blue staining solution (0.05% Alcian blue 8GX (Sigma) in 5% glacial acetic acid) and washed with 5% acetic acid. Stained embryos were incubated in methanol and cleared in a 1:2 mixture of benzyl alcohol/benzyl benzoate.

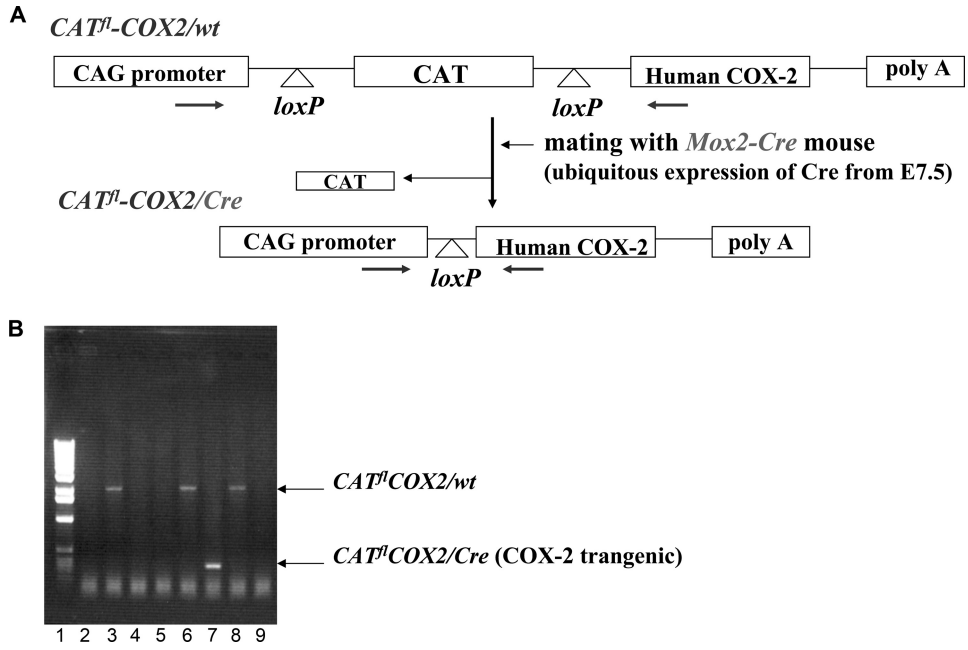

FIGURE 1. *A*, generation of the COX-2 transgenic mouse. Human *COX-2* cDNA was placed between CAG promoter and CAT cDNA. CAT cDNA is flanked by two *lox*P sequences. The mouse that had a synthetic CAG promoter-CAT-COX2-poly(A) construct was generated first and designated as the *CAT*^{fl}*COX2/wt* mouse. A *CAT*^{fl}*COX2/wt* mouse was mated with a *Mox2-Cre* mouse that ubiquitously expressed Cre recombinase. Only in mice that have both COX-2 and Cre (*CAT*^{fl}*COX2/Cre*) will an interfering CAT gene be deleted by recombination at the two *lox*P sites, and COX2 will be expressed. The *arrows* indicate the primer annealing sites for genotyping. *B*, genotyping of COX-2 transgenic mouse. Genomic DNAs from tails of E18.5 fetuses were amplified with the specific primer set. A 300-bp PCR product from the COX-2 transgenic fetus (*CAT*^{fl}*COX2/Cre*) was generated due to Cre-mediated excision of CAT cDNA (*lane 7*). *Lane 1*, 1-kb DNA marker; *lanes 3*, *6*, and *8*, *CAT*^{fl}*COX2/wt*. *Lanes 2, 4, 5,* and *9*, wt/wt or wt/Cre.

Micro-CT Analysis—Numira Biosciences (Irvine, CA) scanned three pairs of non-transgenic control and transgenic littermates using the μCT 40 scanner (ScanCo USA, Southeastern, PA). Samples were prescanned at 10 μm resolution for skeletal morphology and then processed through a series of steps for a proprietary Virtual Histology^{TM} stain for the analysis of soft tissue architecture. Images were acquired with standard parameters of exposure time (300 ms), frames per view (5), and number of views (2000). Density values were in Hounsfield units on a 16-bit scale, using the definition that air is 1000 Hounsfield units and water is 0 Hounsfield units.

Confocal Microscopy—Sections were incubated with primary antibody at 4 °C overnight. Washed sections were incubated in Alexa fluo 488-conjugated goat anti-rabbit IgG (1:2500; Invitrogen) and Alexa fluo 594-conjugated goat anti-mouse IgG (1:2500; Invitrogen) for 30 min. Confocal images were taken on a Zeiss LSM 510 UV a C-Apochromat ×40/1.2 water corrected objective lens, with the pinhole set to yield, an optical slice of 1 μm, and a scan zoom of ×0.7.

RESULTS

Generation of COX-2 Transgenic Mice Using Cre-loxP System and Expression of COX-2 in Transgenic Mice—A diagram of the *COX-2* transgene is shown in Fig. 1*A*. In this construct, the cytomegalovirus early enhancer/chicken β-actin (CAG) promoter was used to direct the expression of the human *COX-2* gene in transgenic mice. A CAT reporter gene flanked by two *lox*P sites was placed between the CAG promoter and the human *COX-2* gene. Upon Cre recombinase-mediated DNA recombination, the CAT gene is excised, and COX-2 is expressed under the CAG promoter. Two independent lines of floxed CAT/*COX-2* mice (herein designated as *CAT*^{fl}*COX2/wt*) were produced, and these mice were crossed with *Mox2-Cre* mice (*Cre/wt*), which ubiquitously express Cre at the early stages of embryonic development (E7.5–E8.5) from the *Mox2* locus (6), to generate the COX-2 transgenic mice (*CAT*^{fl}*COX2/Cre*) and the experimental controls (*wt/wt*, *CAT*^{fl}*COX2/wt*, and *Cre/wt*) in the same litter. The sequences of PCR primers for genotyping were chosen in the CAG promoter and the *COX-2* cDNA (Fig. 1*A*). PCR amplification of genomic DNA using this primer pair generated two different size fragments, depending on the presence of either floxed CAT/*COX-2* allele or recombinant *COX-2* allele. Without Cre-mediated recombination (*CAT*^{fl}*COX2/wt*), PCR amplification generated a 1.8-kb fragment, whereas PCR with genomic DNA from COX-2 transgenic mice (*CAT*^{fl}*COX2/Cre*) produced a 300-bp PCR product due to the excision of CAT cDNA (Fig. 1*B*).

Although floxed CAT/*COX-2* (*CAT*^{fl}*COX2/wt*) or Cre (*Cre/wt*) mice appeared to be normal and were fertile, no COX-2 transgenic mice (*CAT*^{fl}*COX2/Cre*) were obtained, suggesting that the expression of COX-2 may result in an embryonic lethality. Examination of embryos at E10.5, E17.5, and neonates revealed that the transgenic expression of COX-2 is not embryonically lethal, but the transgenic individuals die shortly after birth. When isolated by cesarean section at E18.5, 100% of COX-2 transgenic fetuses died within 5–30 min, indicating that COX-2 expression causes postnatal death. COX-2 transgenic fetuses were identified by a shortened body axis and distended circumference of the thoracic and abdominal areas (Fig. 2*A*). In addition, generalized edema, midfacial hypoplasia (short snout), and occasional umbilical hernia were observed in COX-2 transgenic fetuses. Identical phenotypes were obtained in transgenic fetuses from the two independent lines.

To confirm COX-2 expression in the COX-2 transgenic fetuses, various tissues from E18.5 COX-2 transgenic and non-transgenic control littermates were isolated and analyzed by Western blotting with an antibody that specifically recognizes human COX-2 but not mouse COX-2. Because Cre recombinase is ubiquitously expressed from the *Mox2* locus (6), a widespread expression of COX-2 was expected in the COX-2 transgenic fetus. As shown in Fig. 2*B*, COX-2 was expressed in many tissues from the E18.5 transgenic fetus, including the heart,

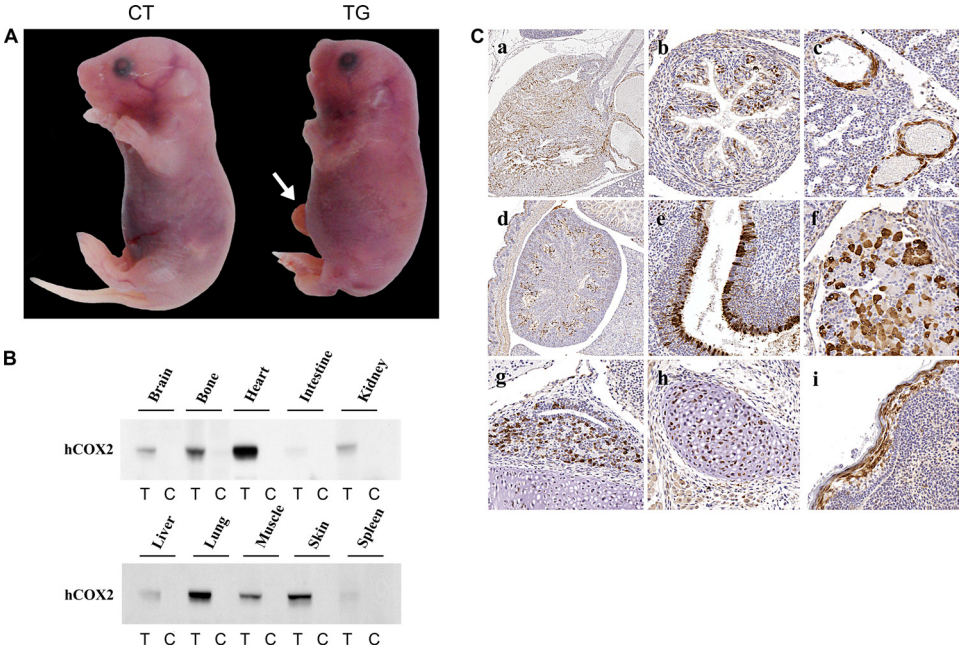

FIGURE 2. *A*, abnormal fetal development in COX-2 transgenic fetus. E18.5 non-transgenic control (*CT*) and COX-2 transgenic (*TG*) littermates were isolated by cesarean section and photographed. COX-2 transgenic fetuses were identified by a shortened body axis and distended circumference of the thoracic and abdominal areas. Generalized edema, mid-facial hypoplasia, and occasional umbilical hernia (*arrow*) were observed in transgenic fetuses. *B*, expression of human COX-2 (*hCOX-2*) in various tissues of transgenic fetuses. Various tissues from E18.5 transgenic (*T*) and control (*C*) littermates were isolated and analyzed by Western blot analysis with antibody that specifically recognizes human COX-2 but not mouse COX-2. *C*, distribution of COX-2 expression in different tissues from the COX-2 transgenic mouse. Paraffin-embedded sections of E18.5 transgenic fetus were stained for COX-2 using a human COX-2-specific antibody. The tissues shown are heart (*a*), intestine (*b*), lung (*c*), kidney (*d*), nasal cavity (*e*), pancreas (*f*), pituitary (*g*), cartilage (*h*), and skin (*i*).

lung, skin, and bone. Immunohistochemical staining for human COX-2 (Fig. 2*C*) confirmed strong expression of the human COX-2 transgene in many tissues, consistent with the results from Western blot analysis. The expression of endogenous (mouse) COX-2 was not detected, whereas endogenous COX-1 was expressed in the tissues examined (supplemental Fig. 1).

Skeletal Malformations in COX-2 Transgenic Fetuses—In order to determine the cause of postnatal death in COX-2 transgenic individuals, micro-CT analysis was conducted with E18.5 control and transgenic littermates ($n = 4$). Micro-CT analysis revealed that COX-2 transgenic fetuses exhibited a small thoracic cavity and a loss of normal spinal curvature (Fig. 3*A*). In addition, the lungs of COX-2 transgenic fetuses were not inflated (Fig. 3*A*), suggesting that postnatal lethality is caused by respiratory failure, which may be partially associated with malformations of the axial skeleton. To obtain a better understanding of the skeletal abnormalities present in COX-2 transgenic fetuses, E18.5 control and transgenic littermates were subjected to skeletal image analysis ($n = 3$). As shown in Fig. 3, *B* and *C*, transgenic fetuses exhibited the most dramatic defects in axial components of the skeletal system. The vertebral columns of transgenic fetuses were severely malformed, resulting in scoliosis and kyphosis. Split ossification centers of the vertebral bodies and fusion of neural arches or vertebral bodies were observed. Hypoplastic vertebrae were present along the vertebral column. The ribs were often thin and discontinuous, and the proximal end of the ribs did not have contact with the vertebral bodies. Alcian blue-Alizarin red staining of the E18.5 fetal skeleton corroborated with these findings ($n = 20$; Fig. 3*D*). Histological analysis (Fig. 3*E*) revealed that vertebral columns of transgenic fetuses exhibited disorganization of regular growth with incomplete development of the articulations between each vertebrae and the absence of the normal orderly maturation of the cartilage into bone. In addition, development of the medullary cavity was reduced or completely absent. These results show that COX-2 expression interferes with the skeletal development, most significantly affecting the development of axial skeleton.

Abnormalities in Cartilage Anlagen of COX-2 Transgenic Embryos—The axial skeleton is formed as a result of endochondral ossification, which is composed of a series of events, including formation of cartilage anlagen, vascularization of blood vessels, and osteoblast differentiation. To determine if COX-2 interferes with the development of the axial skeleton before or after the onset of endochondral ossification, cartilage staining of E13.5 embryos was performed ($n = 6$). At this stage of skeletal development, endochondral skeletal elements, including the axial skeleton, consist of cartilage anlagen, which forms the future skeleton. As shown in Fig. 4, *A* and *B*, disorganization along the axial skeleton was evident in E13.5 transgenic embryos, whereas all vertebral elements were established in control embryos. In transgenic embryos, a slight loss of vertebral curvature was observed, and nearly all vertebral elements were hypoplastic. Additionally, the cartilage precursors of the vertebral body and arch were fused with each other, and the intervertebral disks were malformed. The ribs were discontinuous, and the proximal ends of the ribs were loosely connected to vertebral bodies. These results indicate that the malformations in transgenic embryos occur at an earlier stage of axial skeletal development than the formation of cartilage anlagen.

Patterning and Segmentation of Somites in COX-2 Transgenic Embryos—The vertebral column and ribs originate from the sclerotome, which develops in the somites. The somites bud off from the rostral end of the paraxial mesoderm and undergo differentiation in response to inductive signals from the surrounding tissues. The dorsal part of somites differentiates into dermomyotome, which gives rise to dermis and striated muscles, whereas the ventral part of somites undergoes an epithelial-mesenchymal transition and differentiates into the sclerotome (7, 8). The establishment of cranio-caudal polarity in somites has been shown to be essential for the development of the metameric pattern in vertebrates, and disruption of these processes results in defects of the axial skeleton. Therefore, it is possible that COX-2 causes a loss of cranio-caudal polarity or

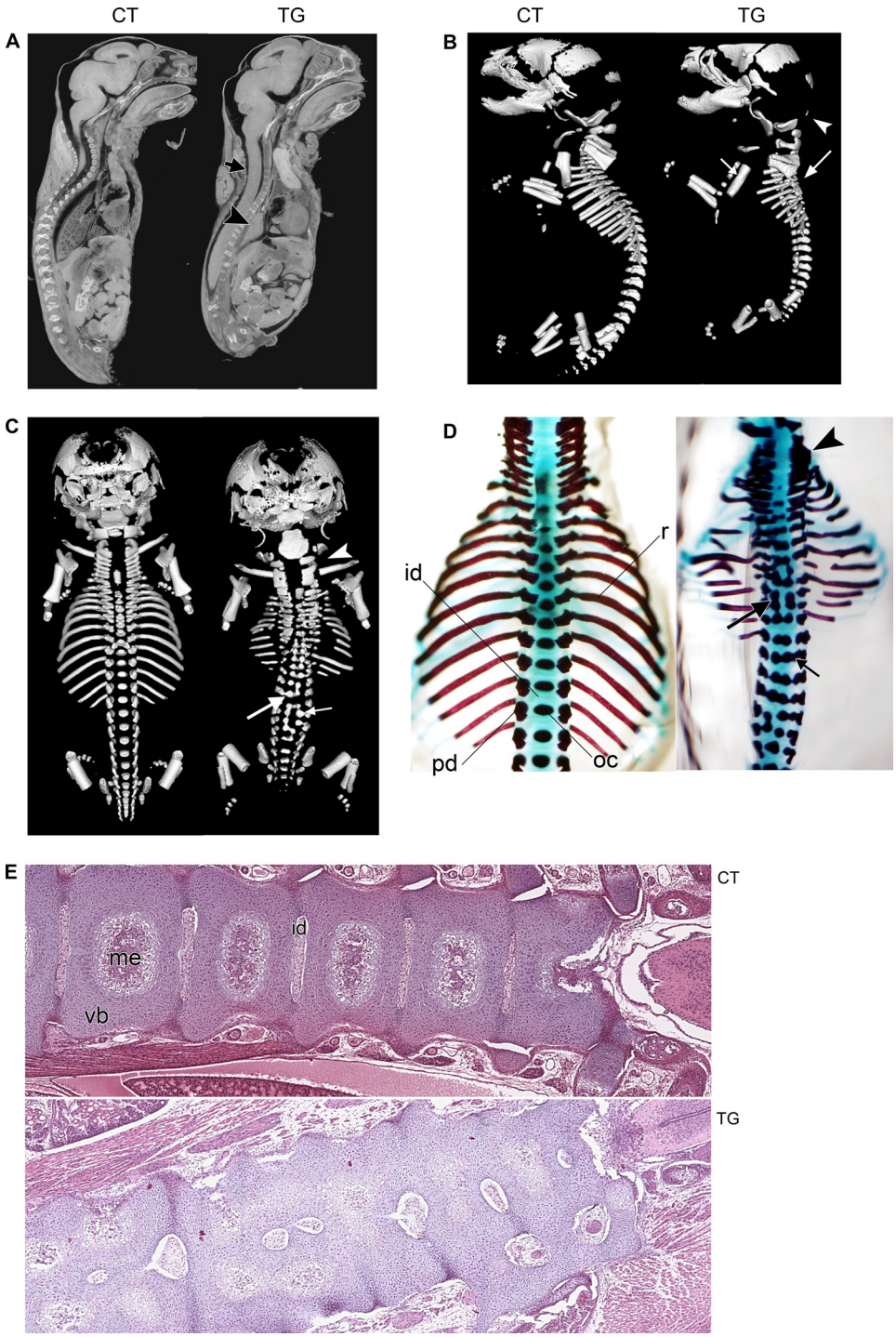

FIGURE 3. *A*, micro-CT image of E18.5 non-transgenic control (*CT*) and COX-2 transgenic (*TG*) littermates in parasagittal orientation. Note the small thoracic cavity, collapsed lung (*arrowhead*), and loss of spinal curvature (*arrow*) in the transgenic fetus. *B*, lateral view of skeletal image analysis of E18.5 non-transgenic control and transgenic littermates. Ossified skeletal elements were visualized. Although the transgenic fetal skeletons exhibited reduced ossification in some of the dorsal cranial skull plates (*arrowhead*), which has a mesodermal origin, the rest of the skull, which is derived from neural crest, appeared normal. The long bones of the limbs were minimally affected except for the absence of deltoid tuberosity on the humerus in all transgenic fetuses (*small arrow*). The tympanic bulla appears to have been displaced caudally. In the transgenic fetus, normal vertebral curvature was lost (*large arrow*) due to malformation of vertebral components. *C*, dorsal view of skeletal image analysis of E18.5 non-transgenic control and transgenic littermates. In COX-2 transgenic fetuses, malformation occurred along the entire vertebral column and rib cage. Split ossification center (*small arrow*), fusion of pedicles with ossification center (*large arrow*), and fusion between pedicles of cervical vertebrae (*arrowhead*) were observed. Ribs were thin and discontinuous. *D*, dorsal view of Alcian blue/Alizarin red staining of E18.5 transgenic and control littermates. Cartilaginous elements are shown in *blue*, and ossified elements are shown in *red*. The forelimbs and shoulder girdles were removed for ease of viewing. Fusion of pedicles to ossification centers (*small arrow*) and dual ossification centers of vertebral bodies and fusion between ossification centers (*large arrow*) were observed. Fusions between pedicles of cervical vertebrae were displayed (*arrowhead*). The ribs were often thin and discontinuous, and the proximal end of the ribs did not contact the vertebral bodies. *id*, intervertebral disk; *oc*, ossification center; *pd*, pedicle; *r*, rib. *E*, hematoxylin/eosin staining of frontal section of E18.5 control and transgenic littermates (magnification, ×4). The *right side* is anterior. Note vertebral fusion and incomplete development of intervertebral disks and medullary cavity. *me*, medullary cavity; *vb*, vertebral body.

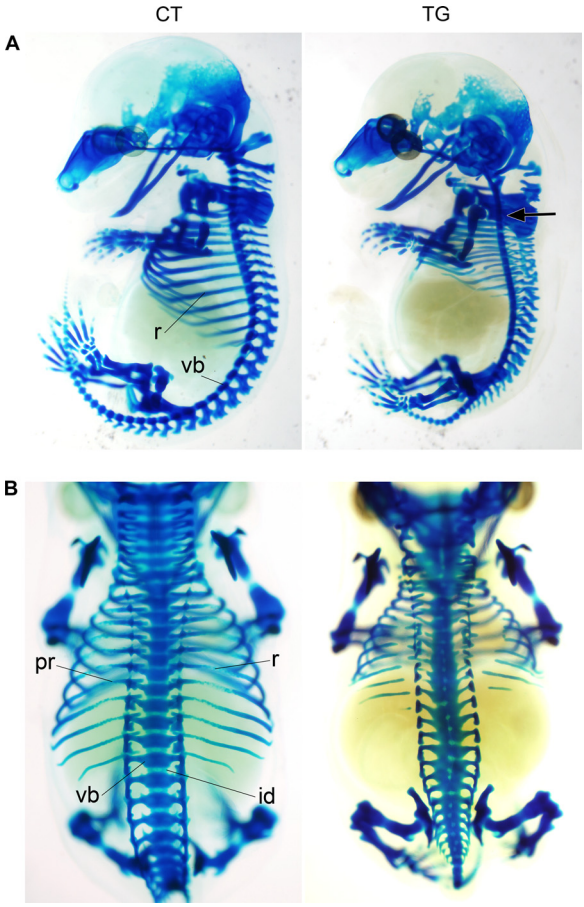

FIGURE 4. **Alcian blue cartilage staining of E13.5 control (*CT*) and transgenic (*TG*) littermates.** A slight loss of vertebral curvature was observed in COX-2 transgenic embryo (*arrow*). The cartilage precursors of entire vertebral components were malformed in the COX-2 transgenic embryo. The cartilaginous precursors of the posterior skull are also reduced. *r*, rib; *vb*, vertebral body; *id*, intervertebral disk; *pr*, proximal rib. *A*, lateral view; *B*, dorsal view.

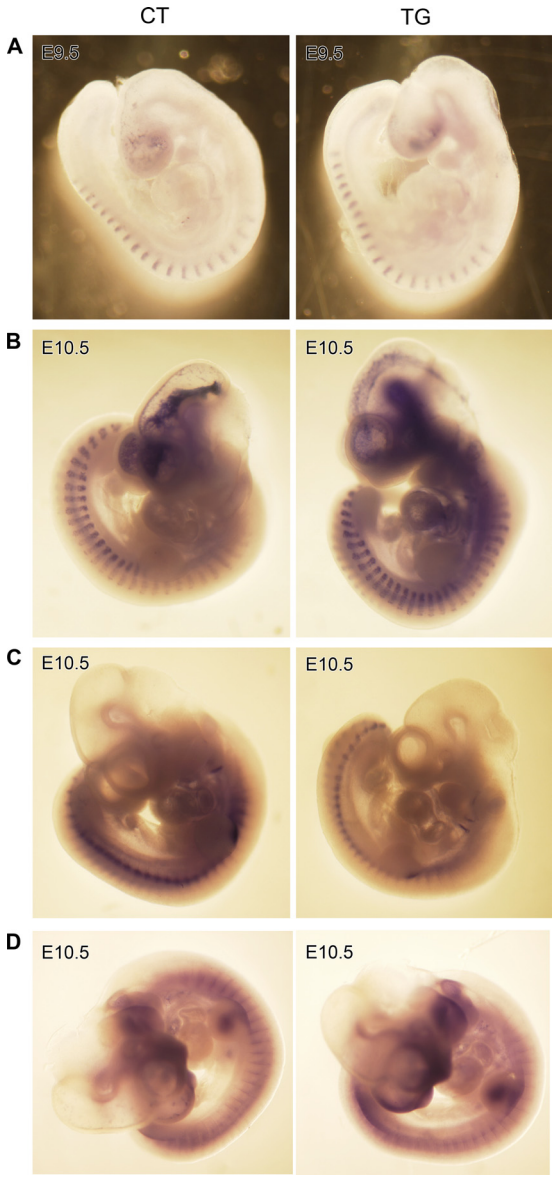

FIGURE 5. **Whole mount *in situ* hybridization of E9.5 (*A*) and E10.5 (*B–D*) control (*CT*) and transgenic (*TG*) embryos.** *Uncx4.1* is expressed in the caudal half of epithelial somite, *Myogenin* in myotome, and *Pax1* and *Sox9* in sclerotome. Although the levels and the patterns of *Uncx4.1* (*A*) and *Myogenin* (*B*) were not altered, the staining intensity of *Pax1* (*C*) and *Sox9* (*D*) was decreased in COX-2 transgenic embryos.

interferes with border formation during somitogenesis. To test this, the expression of markers for somite differentiation was compared in transgenic and control littermates using whole mount *in situ* hybridization. The homeobox gene *Uncx4.1* is expressed in the caudal half of the somite (9), and *Myogenin* is expressed in the myotome of the somite (10) in a metameric pattern. At E9.5, the pattern of *Uncx4.1* staining was evenly spaced in both control and transgenic embryos, and the level of expression was indistinguishable (Fig. 5*A*, $n = 6$), suggesting that cranio-caudal polarity in somites was not disturbed in the transgenic embryos. In addition, the level and pattern of *Myogenin* expression were not altered in E10.5 transgenic embryos (Fig. 5*B*, $n = 6$), suggesting that the myotome development was not affected by COX-2 expression. *Pax1*, a member of the paired box transcription factor family, is expressed in sclerotome (11). As shown in Fig. 5*C*, the level of *Pax1* staining was significantly reduced in E10.5 transgenic embryos, although the pattern of *Pax1* expression was not altered ($n = 6$). In addition, the staining intensity of *Sox9*, an obligatory transcription factor for chondrogenesis, in the sclerotome was also reduced in transgenic embryos (Fig. 5*D*, $n = 6$). These results suggest that somite segmentation is not disturbed but that the development of the sclerotome may be impaired in transgenic embryos.

Reduced Sclerotomal Condensation in COX-2 Transgenic Embryos—The decreased staining of *Pax1* and *Sox9* in transgenic embryos suggests that the expression of these genes is low or that fewer cells are contained in the sclerotome. *Col2a1* (collagen II α1) is expressed in sclerotomal cells of mouse embryos (12, 13) and defines the sclerotome area (14). Therefore, immunohistochemical analysis for *Col2a1* was conducted to determine the number of sclerotomal cells in E10.5 control and transgenic embryos. As shown in Fig. 6, *A* and *B*, the number of *Col2a1*-expressing sclerotomal cells in transgenic embryos was reduced (2.5–3-fold) compared with control embryos. In addition, although the sclerotome of control embryos was organized into cell-dense lateral sclerotome and more diffuse medial sclerotome, this sclerotomal organization was lost in transgenic embryos (Fig. 6*A*). At this stage, COX-2 was ubiqui-

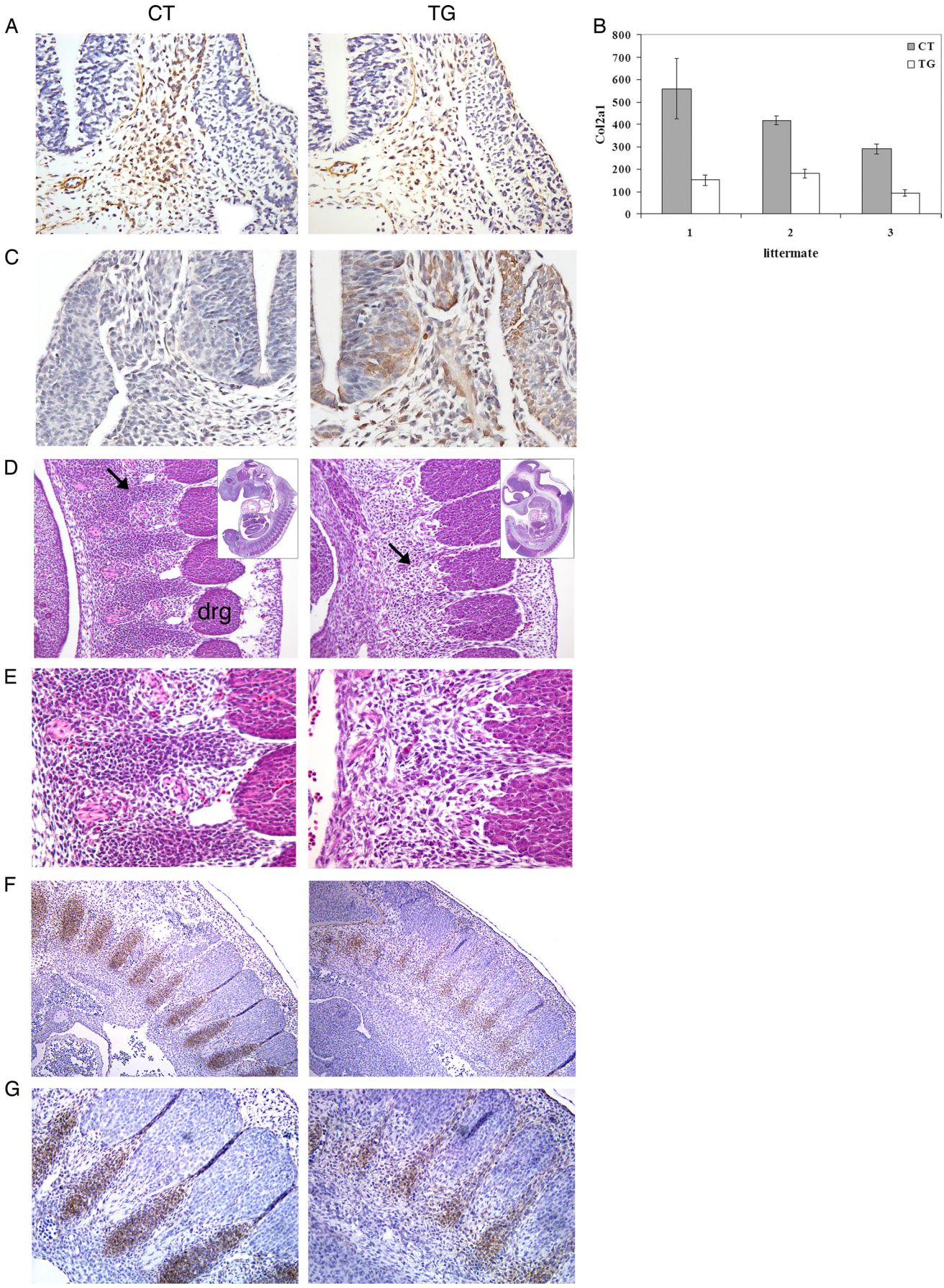
CT
TG
A
B
C
D
E
F
G
drg
800
700
600
500
400
300
200
100
0
Col2a1
CT
TG
1
2
3
littermate

tously expressed in the transgenic embryo, including neural tube, sclerotome, and dermomyotome (Fig. 6*C*). This result suggests that decreased expressions of *Pax1* and *Sox9* in the transgenic embryos may be due to a reduction of cell numbers contained in the sclerotome.

During the development of the axial skeleton, sclerotomal cells condense at the site of future cartilage anlagen and differentiate into chondrocytes. Studies have suggested that hypoplastic or malformed skeletal elements result from a decreased number of cells at the time of mesenchymal condensation (15). Because the number of sclerotomal cells was significantly decreased in transgenic embryos, we examined whether the formation of precartilaginous sclerotomal condensation is altered in transgenic embryos. Histological analysis revealed that precartilaginous sclerotomal condensations were weak or absent in E11.5 transgenic embryos (Fig. 6, *D* and *E*), whereas an alternating pattern of sclerotomal condensation was clearly observed in control littermates. In addition, *Col2a1* has been shown to be expressed in sclerotomal condensations for future vertebral cartilage (12, 13). Immunohistochemical staining of *Col2a1* confirmed that *Col2a1*-expressing sclerotomal condensation was greatly reduced in E11.5 transgenic embryos (Fig. 6, *F* and *G*). These results suggest that sclerotomal condensation for the formation of future cartilage anlagen is impaired in transgenic embryos due to a reduction in the number of sclerotomal cells.

Proliferation and Survival of Sclerotomal Cells in COX-2 Transgenic Embryos—In order to determine the mechanism by which the number of sclerotomal cells was reduced, the differences in proliferation and survival of sclerotomal cells between control and transgenic embryos were examined. To determine the differences in the rate of cell proliferation, immunohistochemical analysis for phosphohistone H3 (Ser^{10}), a mitosis marker, was conducted on serial transverse sections from control and transgenic littermates ($n = 3$) at E9.5. The number of mitotic cells in the sclerotome was not significantly changed between control and transgenic embryos (Fig. 7, *A* and *B*). However, immunohistochemical analysis for cleaved caspase-3, a marker for apoptosis, in the same region revealed that the number of cleaved caspase-3-positive cells was significantly increased in sclerotome of transgenic embryos (Fig. 7, *C* and *D*) but neither in the neural tube (Fig. 7*C*) nor in the embryonic heart (supplemental Fig. 3), suggesting that COX-2 expression selectively interferes with the survival of sclerotomal cells. This notion was further confirmed by TUNEL staining analysis, which showed a 20–30-fold increase in the number of TUNEL-positive cells in the sclerotome of transgenic embryos (supplemental Fig. 2). Whole-mount TUNEL staining analysis revealed that the number of TUNEL-positive cells increased along the entire rostro-caudal axis of transgenic embryos, whereas few TUNEL-positive cells were observed along the rostral part of the vertebral axis (Fig. 7, *E* and *F*). Together, these results suggest that the reduced number of sclerotomal cells, due to an increased apoptosis, is responsible for the loss of sclerotomal condensation in transgenic embryos, leading to defective formation of cartilage anlagen.

Increased Expression of p53 in Sclerotomal Cells of COX-2 Transgenic Embryos—Apoptosis is a complex process in which various signaling pathways interact with each other. Among these, p53 plays a pivotal role in the cellular response to environmental and physiological stresses and is known as a major mediator of growth arrest and apoptosis. In order to provide the possible mechanism by which COX-2 induces sclerotomal apoptosis, immunohistochemical analysis for p53 was conducted. Surprisingly, immunohistochemical staining for p53 revealed the strong accumulation of p53 (30–50-fold increase) in the sclerotome of transgenic embryos (Fig. 8, *A* and *B*) but not in the neural tube (Fig. 8*A*). This result suggests that COX-2 induces an increase in p53 protein, which may contribute to sclerotome-specific apoptosis.

To examine if COX-2 is directly involved in increased expression of p53, the co-localization of COX-2 and p53 expression was determined. COX-2 is a key enzyme for the synthesis of prostaglandins that act in an autocrine and/or paracrine manner on target cells. Prostaglandin levels, as well as COX-2 activity, were increased as expected from the increase in COX-2 expression in the transgenic fetuses (data not shown). Consistent with this notion, confocal microscopic analysis revealed that some cells in the sclerotome of transgenic embryos expressed both COX-2 and p53, whereas other cells only expressed p53 (Fig. 8, *C* and *D*). This result suggests that the increase in the p53 level may be mediated by the increased level of prostaglandins. No sclerotomal cells in the control embryos were positively stained for p53 and COX-2 (Fig. 8*C*).

DISCUSSION

Many studies in both animal models and human subjects have shown that COX/prostaglandins are important mediators of various physiological and pathological processes. Although studies have previously implicated the possible association of COX-2/prostaglandins with embryonic malformation (3–5), the direct effect of COX-2 on fetal malformations has not been examined. In this report, we hypothesized that aberrant COX-2 expression during a critical period of embryogenesis may interfere with fetal development. Indeed, COX-2 transgenic fetuses exhibited severe defects in axial skeleton and died shortly after birth due to respiratory distress. Our results show that (i) the number of apoptotic cells in the sclerotome is greatly increased, (ii) the number of sclerotomal cells is reduced, (iii) the formation of precartilaginous mesenchymal condensation is impaired, and (iv) the formation of cartilage anlagen is defective in COX-2 transgenic embryos. In conclusion, the malformation of

FIGURE 6. *A*, immunohistochemical staining of *Col2a1* on transverse sections of E10.5 control (*CT*) and transgenic (*TG*) littermates (magnification, ×20). The sclerotome of the transgenic embryo contained fewer cells compared with control embryo, and the organization of lateral and medial sclerotome was lost in transgenic embryo. *B*, graphical presentation of Col2a1-positive cells in the sclerotome from serial sections of control and transgenic littermates ($n = 3$). *Error bars*, S.D. *C*, immunohistochemical staining of human COX-2 on transverse sections of E10.5 control (*CT*) and transgenic (*TG*) littermates (magnification, ×20). *D*, histological analysis of sclerotomal condensations in E11.5 embryos. In transgenic embryos, precartilaginous sclerotomal condensations (*arrow*) were weak. *drg*, dorsal root ganglion (magnification, ×15.5). *E*, a higher magnification view of *D* (magnification, ×28). *F*, immunohistochemical staining of *Col2a1* on parasagittal sections of E11.5 control and transgenic littermates (magnification, ×10). *G*, a higher magnification view of *F* (magnification, ×20).

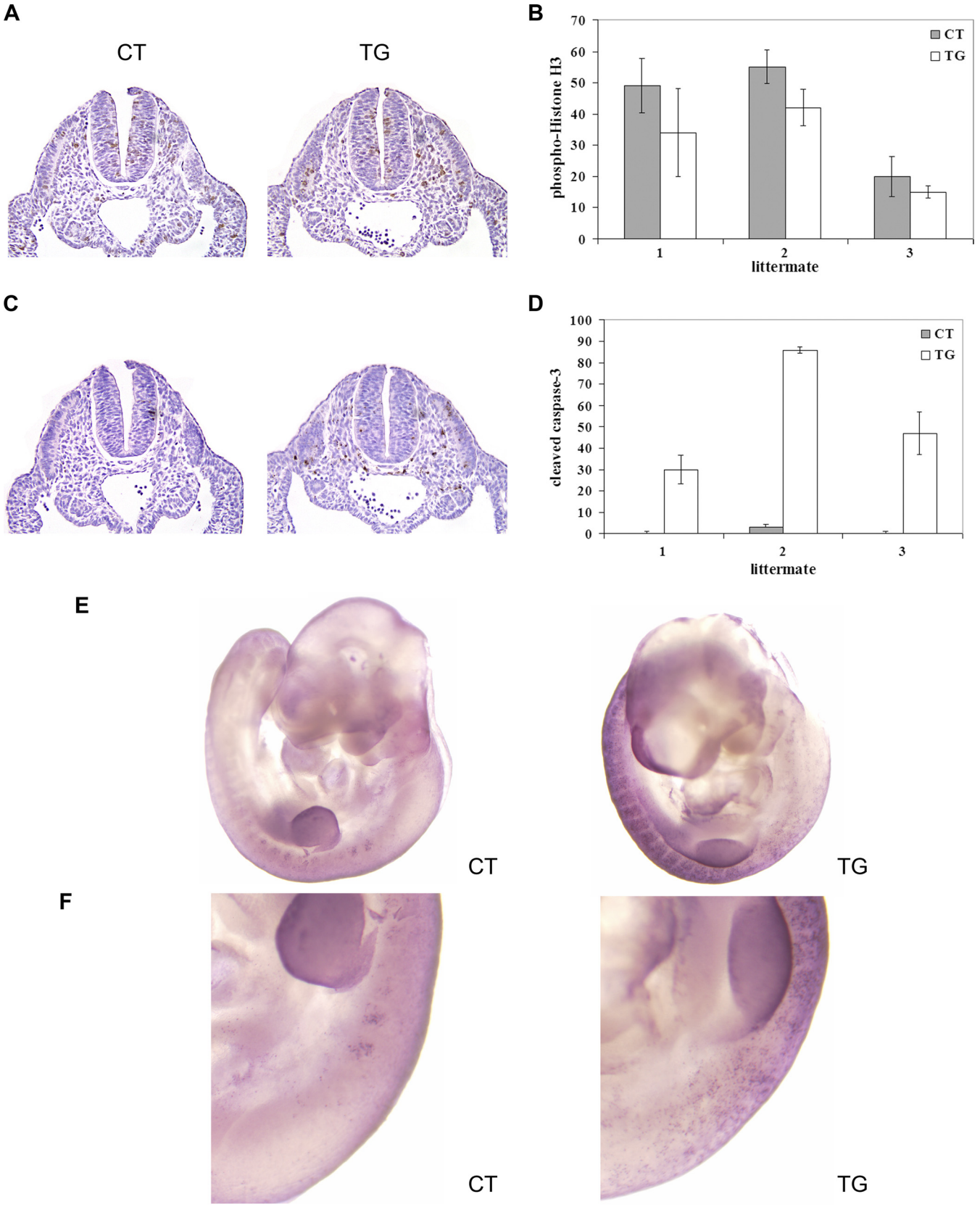

FIGURE 7. *A*, immunohistochemical staining of phosphohistone H3 (Ser[10]), a mitosis marker, on transverse sections of E9.5 control (*CT*) and transgenic (*TG*) littermates (magnification, ×10). *B*, graphical presentation of phosphohistone H3-positive cells in the sclerotome from serial sections of control and transgenic littermates ($n = 3$). *Error bars*, S.D. *C*, immunohistochemical staining of cleaved caspase-3, a marker for apoptosis, on transverse sections of E9.5 control and transgenic littermates (magnification, ×10). *D*, graphical presentation of cleaved caspase-3-positive cells in the sclerotome from serial sections of control and transgenic littermates ($n = 3$). *E*, whole-mount TUNEL staining of E10.5 control and transgenic littermates ($n = 3$). The forelimb region is shown in *F*. The *upper side* is anterior, and apoptotic nuclei appear as *dark blue dots*.

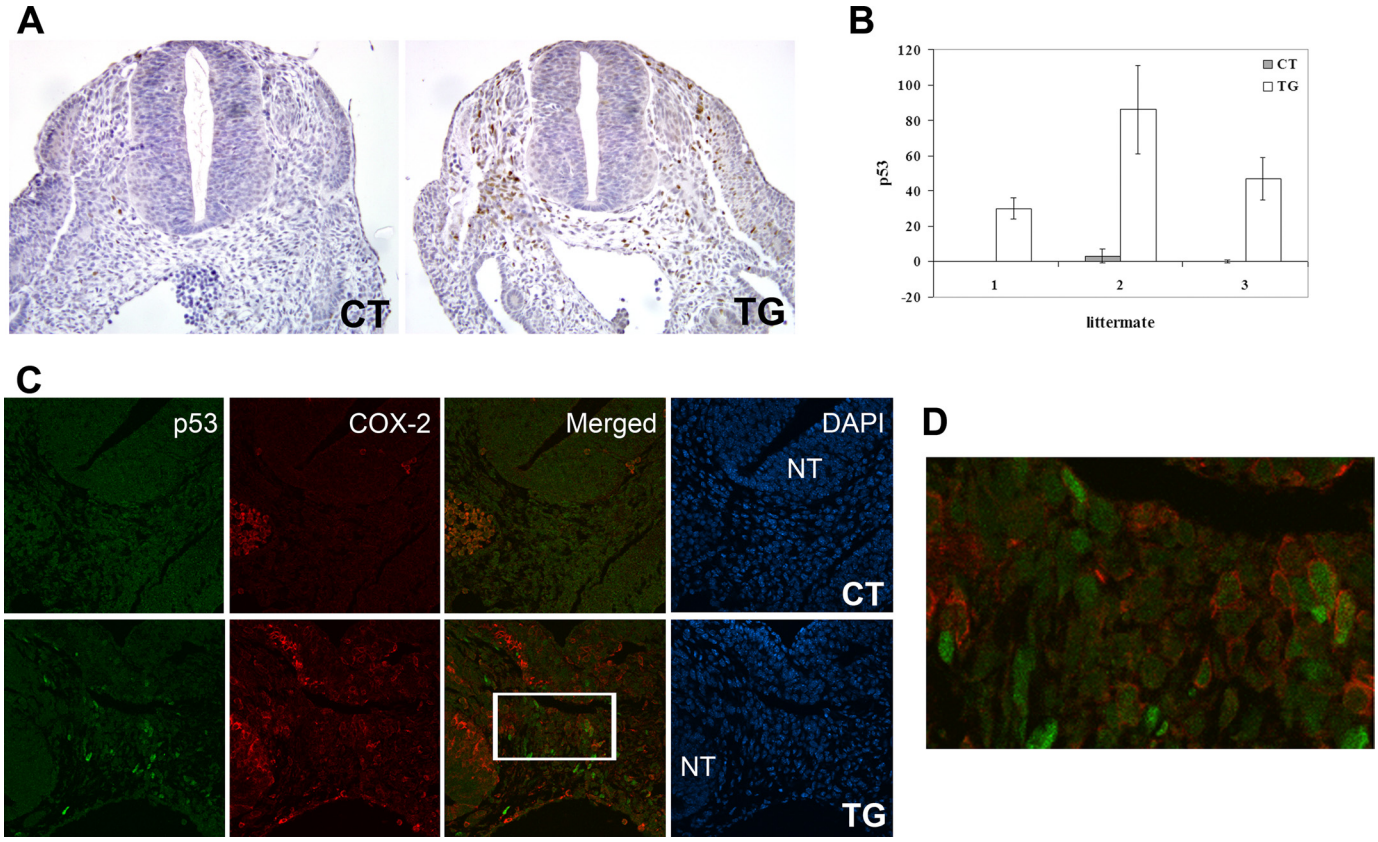

FIGURE 8. *A*, immunohistochemical staining of p53 on transverse sections of E9.5 control (*CT*) and transgenic (*TG*) littermates (magnification, ×10). *B*, graphical presentation of p53-positive cells in the sclerotome from serial sections of control and transgenic littermates ($n = 3$). *Error bars*, S.D. *C*, immunofluorescence staining of p53 (*green*) and COX-2 (*red*) on transverse sections of E10.5 control and transgenic littermates using confocal microscopy (magnification, ×40). Nuclei were stained with 4′,6-diamidino-2-phenylindole (*DAPI*) (*blue*). *NT*, neural tube. *D*, higher magnification view of the *boxed area* in the sclerotome of the transgenic embryo in *C*.

the axial skeleton in COX-2 transgenic fetuses probably originates from increased sclerotomal apoptosis. Our results demonstrate that the aberrant expression of COX-2 during embryonic development is teratogenic.

A number of studies have shown that COX-2 expression renders cells resistant to apoptosis (16, 17). In contrast, our study provides evidence that COX-2 expression results in increased sclerotomal apoptosis. In E9.5–E10.5 COX-2 transgenic embryos, COX-2 is expressed ubiquitously. However, an increased apoptosis was not observed ubiquitously. For example, the number of apoptotic cells in the embryonic heart (supplemental Fig. 3) or neural tube, where COX-2 was abundantly expressed, was not affected by transgenic expression of COX-2. Therefore, it appears that increased sclerotomal apoptosis is a cell-specific response to COX-2 expression. Although the mechanism underlying the selective induction of apoptosis by COX-2 remains to be determined, it has been shown that excessive cell death is one of the most critical events in fetal malformations and that various teratogens induce apoptosis in their target organs. Our results are consistent with this notion and emphasize the importance of controlled apoptosis in embryonic development.

In certain types of cancer, high levels of COX-2 expression are correlated with the accumulation of p53 (18–20). Although p53 has been shown to up-regulate or down-regulate COX-2 expression, depending on the cellular context, the modulation of p53 level by COX-2 is not clearly understood. Our finding that COX-2 expression is associated with an increased level of p53 in the sclerotome of transgenic embryos suggests that COX-2 signaling may act upstream of p53 and positively regulate the level of p53. It has been shown that PGE_2 increases p53 activity but not p53 levels in human synovial fibroblasts by inducing serine 15 phosphorylation of p53 in a p38 kinase-dependent manner (21). However, we were not able to find an increase in the level of p38 phosphorylation in the sclerotome of COX-2 transgenic embryos, suggesting that p38 is not responsible for the induction of p53. In addition to the generation of prostaglandins, COX-2 has been known to induce genomic instability (22) and generate reactive oxygen species (23), which increase cellular p53. Although it is not clear how COX-2 expression is related to an increase in p53, induction of p53 in the sclerotome may be more sensitive to the elevated level of COX-2 or prostaglandins. Alternatively, it may be possible that COX-2 modulates p53 via the regulation of other signaling pathways. Sclerotomal survival is dependent on many signaling molecules, such as Shh, BMPs, Wnts, and Fgfs from surrounding structures, including neural tube, notochord, and surface epithelium (24). These signaling molecules have been shown to interact with p53 (25–28). Thus, COX-2 expression may alter the expression of these signaling molecules from surrounding structures or the sclerotomal response to these signaling molecules. Interestingly, many

signals that increase COX-2 expression also induce p53 (29). Therefore, COX-2 may positively regulate p53 to protect the cell from DNA damage during inflammation or to eliminate irreversibly damaged cells. Future studies will be aimed at determining the mechanism by which COX-2 regulates sclerotomal apoptosis and p53.

Although COX-2 and p53 are co-expressed in some cells in the sclerotome of transgenic embryos (Fig. 8, *C* and *D*), the staining pattern of COX-2 and cleaved caspase-3 are not overlapped (supplemental Fig. 4). However, the cells positive for cleaved caspse-3 are in the terminal phase of apoptotic cells or apoptotic bodies (Fig. 7*C* and supplemental Fig. 4), as histologically characterized by cell shrinkage and pyknotic nuclei. Although p53 is involved in the initiation phase of the apoptosis, the activation of caspase-3 is responsible for the final phase of apoptosis. Furthermore, the activation of caspase results in the degradation of cellular proteins during apoptosis. Thus, we speculate that COX-2 levels in cleaved caspase-3-positive apoptotic cells may be below the level of detection by immunohistochemistry. In addition, sclerotomal proliferation is not altered in COX-2 transgenic embryos (Fig. 6*B*). In agreement with this result, we did not find a consistent staining pattern of COX-2 and phospho-H3 (data not shown).

Many types of human congenital abnormalities involving the axial skeleton have been described in the literature (30, 31). In addition, these congenital abnormalities are often accompanied by other complications, including the cardiopulmonary, genitourinary, and nervous systems. However, the etiology remains to be determined in most of axial skeletal abnormalities. COX-2 transgenic fetuses exhibit a broad spectrum of characteristic features observed in malformations of the human axial skeleton, such as dwarfism, scoliokyphosis, and rib cage defects. COX-2 is expressed during the early stages of human embryonic development (32) and in fetal membranes throughout pregnancy (33). Because COX-2 expression can be induced by such diverse stimuli, including inflammation, infection, and environmental contaminants, aberrant COX-2 expression at a critical period during embryonic development may be responsible for some of the skeletal defects of unknown etiology in humans.

Increased COX-2 expression is observed in cartilages from osteoarthritis patients (34) and in ankylosing spondylitis (35). Although the functional significance of COX-2 overexpression in initiation or propagation of osteoarthritis or ankylosing spondylitis is currently not known, our findings that the aberrant COX-2 expression interferes with skeletal development suggest that COX-2 may play a pivotal role in pathogenesis of these diseases. In addition, COX-2 has been shown to be involved in bone repair (36), suggesting that COX-2 also plays an important role in the homeostasis of adult skeleton.

It is widely thought that the coordinated interaction between gene and environment is critical in normal embryonic development and that environmental factors that disturb normal embryonic signaling have a potential to result in malformations in the embryo. Upon extensive examination of the literature, we did not find any reference to studies investigating the level of COX-2 expression in fetal malformations. However, this may be due to the fact that the role of COX-2 during malformations has not been previously speculated. Our study suggests that COX-2 may be a previously unrecognized mediator of congenital abnormalities.

Acknowledgments—We thank Drs. Robert Maronpot, Kathy Sulik, and Arthur Aylswoth for constructive comments and helpful suggestions. We thank Justin Kosak for comments and assistance in manuscript preparation. We acknowledge Elizabeth Ney for image scanning and expert preparation of the figures.

REFERENCES

1. Stanfield, K. M., Bell, R. R., Lisowski, A. R., English, M. L., Saldeen, S. S., and Khan, K. N. (2003) *Birth Defects Res. A Clin. Mol. Teratol.* **67,** 54–58
2. Loftin, C. D., Trivedi, D. B., Tiano, H. F., Clark, J. A., Lee, C. A., Epstein, J. A., Morham, S. G., Breyer, M. D., Nguyen, M., Hawkins, B. M., Goulet, J. L., Smithies, O., Koller, B. H., and Langenbach, R. (2001) *Proc. Natl. Acad. Sci. U.S.A.* **98,** 1059–1064
3. Parman, T., and Wells, P. G. (2002) *FASEB J.* **16,** 1001–1009
4. Randall, C. L., Becker, H. C., and Anton, R. F. (1991) *Alcohol Clin. Exp. Res.* **15,** 673–677
5. Randall, C. L., Anton, R. F., Becker, H. C., Hale, R. L., and Ekblad, U. (1991) *Teratology* **44,** 521–529
6. Tallquist, M. D., and Soriano, P. (2000) *Genesis* **26,** 113–115
7. Christ, B., Huang, R., and Wilting, J. (2000) *Anat. Embryol.* **202,** 179–194
8. Saga, Y., and Takeda, H. (2001) *Nat. Rev. Genet.* **2,** 835–845
9. Mansouri, A., Yokota, Y., Wehr, R., Copeland, N. G., Jenkins, N. A., and Gruss, P. (1997) *Dev. Dyn.* **210,** 53–65
10. Montarras, D., Chelly, J., Bober, E., Arnold, H., Ott, M. O., Gros, F., and Pinset, C. (1991) *New Biol.* **3,** 592–600
11. Deutsch, U., Dressler, G. R., and Gruss, P. (1988) *Cell* **53,** 617–625
12. Zhao, Q., Eberspaecher, H., Lefebvre, V., and De Crombrugghe, B. (1997) *Dev. Dyn.* **209,** 377–386
13. Ng, L. J., Wheatley, S., Muscat, G. E., Conway-Campbell, J., Bowles, J., Wright, E., Bell, D. M., Tam, P. P., Cheah, K. S., and Koopman, P. (1997) *Dev. Biol.* **183,** 108–121
14. Peters, H., Wilm, B., Sakai, N., Imai, K., Maas, R., and Balling, R. (1999) *Development* **126,** 5399–5408
15. Mariani, F. V., and Martin, G. R. (2003) *Nature* **423,** 319–325
16. Tsujii, M., and DuBois, R. N. (1995) *Cell* **83,** 493–501
17. Cao, Y., and Prescott, S. M. (2002) *J. Cell. Physiol.* **190,** 279–286
18. Ristimäki, A., Sivula, A., Lundin, J., Lundin, M., Salminen, T., Haglund, C., Joensuu, H., and Isola, J. (2002) *Cancer Res.* **62,** 632–635
19. Legan, M., Luzar, B., Marolt, V. F., and Cor, A. (2006) *World J. Gastroenterol.* **12,** 3425–3429
20. Hermanova, M., Trna, J., Nenutil, R., Dite, P., and Kala, Z. (2008) *Eur. J. Gastroenterol. Hepatol.* **20,** 732–739
21. Faour, W. H., He, Q., Mancini, A., Jovanovic, D., Antoniou, J., and Di Battista, J. A. (2006) *J. Biol. Chem.* **281,** 19849–19860
22. Singh, B., Cook, K. R., Vincent, L., Hall, C. S., Berry, J. A., Multani, A. S., and Lucci, A. (2008) *J. Surg. Res.* **147,** 240–246
23. Xu, Z., Choudhary, S., Voznesensky, O., Mehrotra, M., Woodard, M., Hansen, M., Herschman, H., and Pilbeam, C. (2006) *Cancer Res.* **66,** 6657–6664
24. Monsoro-Burq, A. H. (2005) *Int. J. Dev. Biol.* **49,** 301–308
25. Yang, X., Klein, R., Tian, X., Cheng, H. T., Kopan, R., and Shen, J. (2004) *Dev. Biol.* **269,** 81–94
26. Stecca, B., and Ruiz i Altaba, A. (2009) *EMBO J.* **28,** 663–676
27. Levina, E., Oren, M., and Ben-Ze'ev, A. (2004) *Oncogene* **23,** 4444–4453
28. Fukuda, N., Saitoh, M., Kobayashi, N., and Miyazono, K. (2006) *Oncogene* **25,** 3509–3517
29. de Moraes, E., Dar, N. A., de Moura Gallo, C. V., and Hainaut, P. (2007) *Int. J. Cancer* **121,** 929–937

30. Tyl, R. W., Chernoff, N., and Rogers, J. M. (2007) *Birth Defects Res. B Dev. Reprod. Toxicol.* **80,** 451–472
31. Kaplan, K. M., Spivak, J. M., and Bendo, J. A. (2005) *Spine J.* **5,** 564–576
32. Wang, H., Wen, Y., Mooney, S., Behr, B., and Polan, M. L. (2002) *J. Clin. Endocrinol. Metab.* **87,** 2629–2634
33. Slater, D., Dennes, W., Sawdy, R., Allport, V., and Bennett, P. (1999) *J. Mol. Endocrinol.* **22,** 125–130
34. Amin, A. R., Attur, M., Patel, R. N., Thakker, G. D., Marshall, P. J., Rediske, J., Stuchin, S. A., Patel, I. R., and Abramson, S. B. (1997) *J. Clin. Invest.* **99,** 1231–1237
35. Siegle, I., Klein, T., Backman, J. T., Saal, J. G., Nüsing, R. M., and Fritz, P. (1998) *Arthritis Rheum.* **41,** 122–129
36. Zhang, X., Schwarz, E. M., Young, D. A., Puzas, J. E., Rosier, R. N., and O'Keefe, R. J. (2002) *J. Clin. Invest.* **109,** 1405–1415